Effect of Thiosulfate on Corrosion Behavior and Passive Films of Duplex Stainless Steel 2205 in Chloride Solutions

Jiantao Zhang, Xiaojun Hu[*], Kuochih Chou

State Key Laboratory of Advanced Metallurgy, University of Science and Technology Beijing, Beijing 100083, P.R. China
[*]E-mail: huxiaojun@ustb.edu.cn

The effect of $S_2O_3^{2-}$ on the corrosion behavior and passive films of duplex stainless steel 2205 in a Cl^- -containing environment was investigated by potentiodynamic polarization, electrochemical impedance spectroscopy, Mott-Schottky measurements and XPS composition analysis. The results show that the addition of $S_2O_3^{2-}$ decreased the pitting potential of duplex stainless steel 2205 in Cl^--containing solutions. The corrosion resistance of passive films was influenced by the concentration of $S_2O_3^{2-}$ in Cl^--containing solutions, but the exhibited n-type and p-type semiconductor characteristics were not affected. The modified stability and the variation in donor and acceptor densities of the passive film with the concentration of $S_2O_3^{2-}$ were detected. The primary components of the passive films on duplex stainless steel 2205 in a $Cl^- $-$S_2O_3^{2-}$ solution were Cr-oxides and Fe-oxides or hydroxides with small amounts of Ni and Mo oxides.

1. INTRODUCTION

Duplex stainless steel is an important member of the stainless steels. It not only has the commonalities of stainless steels but also has its own unique advantages, combining the excellent toughness of austenitic steel with the high strength and the resistance to chloride ion of the ferrite phase [1-4]. Therefore, duplex stainless steels have been increasingly used in various environments such as marine construction, the petroleum and chemical industries, power plants, and the pulp and paper industry [5-7].

Pitting is one of the well-known serious localized types of corrosion of duplex stainless steel in a service environment. The high corrosion resistance is primarily attributed to the passive films formed on the surface of duplex stainless steels in aggressive solutions. For this reason, passivation is a question of considerable technical and economic importance [8]. The corrosion resistance of passive films is

determined by their properties that are strongly affected by various internal factors such as alloy composition and microstructure and by environmental conditions such as aggressive ions, pH, and temperature [9-11]. Studies have shown that pitting corrosion is mainly caused by aggressive Cl^- ions and when other ions are present in the solution, the corrosion behavior will be seriously affected [12]. Thiosulfate exists in many engineering environments and synergizes with Cl^- to affect the corrosion behavior of stainless steels. In recent years, the pitting corrosion of stainless steels in thiosulfate-containing solutions has been investigated by many researchers. Cui and Chen [13] studied the passivation behavior and surface chemistry of 2507 super duplex stainless steel in acidified artificial seawater containing thiosulfate. They pointed out that thiosulfate promoted the dissolution process of the passive film in seawater and resulted in higher passive current density and lower polarization resistance. Xia [14] indicated that when the concentration of the thiosulfate ions increases, the semiconductivity of the passive film on Alloy 800 is converted from the n-type to the p-type in 0.1 M chloride solutions. Wu [15] observed the combined effect between chloride and thiosulfate on the pitting corrosion of UNS N08800 at a high anodic potential. Frankel [16] revealed that thiosulfate promoted both cathodic and anodic reactions of X65 steel and that corrosion proceeded with the formation of an iron sulfide film.

However, there are still few studies on the corrosion and passive behavior of duplex stainless steel in a $Cl^- \text{-} S_2O_3^{2-}$ environment. In the present work, we aim to understand the effect of $S_2O_3^{2-}$ on the corrosion behavior and properties of the passive films on duplex stainless steel 2205 in chloride solutions.

2. EXPERIMENTAL

2.1 Materials

The experimental alloy for the present study was duplex stainless steel 2205. The chemical composition of the material was (wt.%): C, 0.015; Cr, 22.34; Ni, 5.24; Mo, 3.21; Mn, 1.48; Si, 0.49; P, 0.025; S, 0.005; N, 0.171; Fe, balance. The alloy specimens for measurement were cut and solution annealed for 10 min per 1 mm thickness at 1050 ℃, followed by water quenching.

Table 1. Test solutions and the corresponding concentration ratio of chloride to thiosulfate in 3.5 wt.% NaCl solutions.

Concentration of thiosulfate ($C_{S_2O_3^{2-}}$): (mol·L^{-1})	$C_{Cl^-}/C_{S_2O_3^{2-}}$	pH
0	$+\infty$	6.82
0.05	12.4	6.81
0.1	6.2	6.83
0.5	1.2	6.82

All surfaces of the samples required removal of the oxide layer. Specimens for electrochemical measurements were joined with a copper wire through conductive silver and then mounted with epoxy resin. The working side of the specimens with an exposed area of 1 cm^2 was mechanically ground with silicon carbide emery papers to 3000 grit, polished with diamond paste to 0.5 μm, ultrasonically rinsed in ethanol for 10 min, and dried in warm air.

The test solutions are 3.5 wt.% NaCl containing various concentrations of $Na_2S_2O_3$ as listed in Table 1. All the solutions were prepared using scientific-grade reagents in distilled water and were used immediately after their preparation.

2.2 Electrochemical Measurements

Electrochemical tests were carried out using a Princeton VersaSTAT 3 electrochemical system, which comprised a traditional corrosion system with a three-electrode cell under naturally aerated conditions at room temperature. A saturated calomel reference electrode (SCE) was connected to the cell via a Luggin capillary filled with a salt bridge as a reference electrode and a platinum plate was used as a counter electrode.

At the beginning of each test, the specimens were pretreated cathodic reduction any of the oxides surface on the duplex stainless steel at -0.8 V_{SCE} for 30 min to improve the reproduction of the experiments. The specimen was then left to corrode freely for approximately 30 min, which will reach a stable open circuit potential (OCP) for all tests. The potentiodynamic polarization curves started from –0.8 V_{SCE} to transpassive potential and were recorded at a rate of 0.5 mV s^{-1}. EIS tests were performed at a steady-state open circuit potential and varied from 100 kHz down to 10 mHz, with a frequency of 10 points per decade using an AC sine signal at an amplitude of 10 mV. Zview software was employed for analysis of the measured EIS data. Mott-Schottky measurements were scanned from -0.8 V_{SCE} to 1.4 V_{SCE} in the anodic direction at a step height of 15 mV and a frequency of 1 kHz.

The electrochemical experiments were repeated at least two times to ensure that the obtained data were reproducible.

2.3 X-ray Photoelectron Spectroscopy

The chemical analysis of the passive films on duplex stainless steel 2205 after potentiostatic polarization for 8 h was performed by XPS using a Thermo ESCALAB 250XI spectrometer with a pass energy of 20 eV and a monochromatic Al Kα radiation source. The spectrum results were fitted using XPSPEAK software which contains the Shirley background subtraction and Gaussian-Lorentzian tail function.

3. RESULTS AND DISCUSSION

3.1 Analysis of Potentiodynamic Polarization Behavior

Figure 1 illustrates the potentiodynamic polarization curves of duplex stainless steel 2205 in 3.5 wt.% NaCl solution containing various concentrations of $Na_2S_2O_3$ ranging from 0 to 0.5 M. The $S_2O_3^{2-}$

added to 3.5 wt.% NaCl solution decreased the pitting potential of duplex stainless steel 2205. The pitting potential was higher in the solution containing only NaCl, and repassivation occurred when the metastable pitting of the passive film occurred. The addition of $S_2O_3^{2-}$ to neutral 3.5 wt.% NaCl solution decreased the breakdown potential from 1.059 V_{SCE} to 0.878 V_{SCE}, indicating that $S_2O_3^{2-}$ played a detrimental effect on passive film breakdown. However, when the concentration of Na₂S₂O₃ in the solution was further increased, the pitting potential did not change significantly.
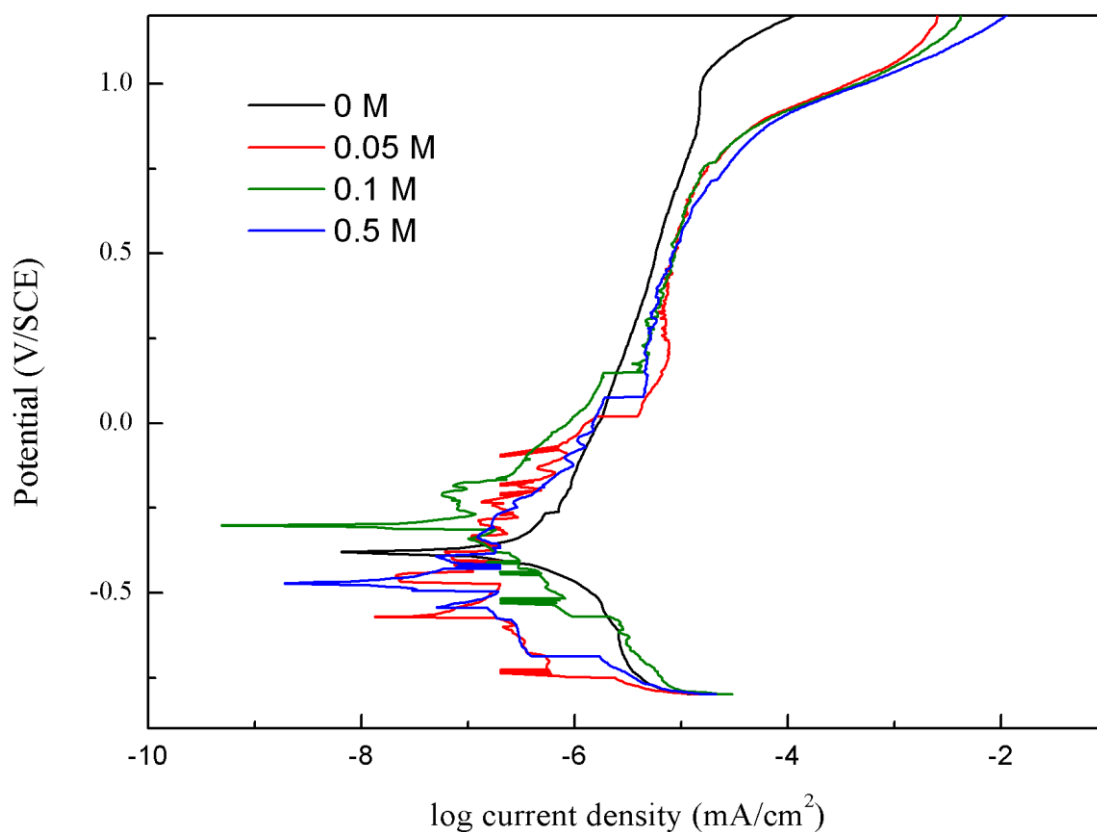

Figure 1. Potentiodynamic polarization curves of duplex stainless steel 2205 in 3.5 wt.% NaCl solution containing various concentrations of thiosulfate

It is worth noting that the current densities were lower than those of the chloride-only solution at low potential, as the surface of the stainless steel remained passive, and the Cl⁻ and $S_2O_3^{2-}$ ions competed for adsorption on the surface of the stainless steel. When the potential was raised, the passive current densities increased for all solutions and remained approximately 10^{-5} A·cm⁻², revealing that the dissolution rate of the passive films increased. As a result, the films became thinner and corrosion resistance became weaker. It was confirmed that the acceleration of the anodic process was responsible for the decrease in the corrosion potential. At high anodic potential, once the aggressive Cl⁻ in the solution caused the collapse of the passive film and induced metastable pitting initiation, the adsorbed $S_2O_3^{2-}$ on the bare surface of matrix prevented the repassivation and inhibited the further formation of a film [17]. In addition, $S_2O_3^{2-}$ was reduced to S^{2-} and formed FeS, as the Fe and Ni have a large affinity

for S species [18,19]. Therefore, the products acted as cathodes of the stainless steel matrix in solution, causing galvanic corrosion and catalyzing anodic dissolution [8,20].

3.2 Electrochemical Impedance Spectroscopy Analysis

The electrochemical impedance spectroscopy measurements were carried out to investigate the electrochemical behavior of the passive films formed on the duplex stainless steel 2205. The open-circuit impedances of films on duplex stainless steel 2205 formed at the polarization potential of 0.2 V_{SCE} for 2 h in NaCl solutions containing various $Na_2S_2O_3$ concentrations was measured. The effect of the concentration of $Na_2S_2O_3$ on the experimental spectra is shown in Figure 2. All the Nyquist plots were characterized as unfinished semi-arcs at low frequency, indicating a similar passive mechanism. It can be seen that when 0.05 M $Na_2S_2O_3$ was added to the 3.5 wt.% NaCl solution, the arc radius decreased significantly.
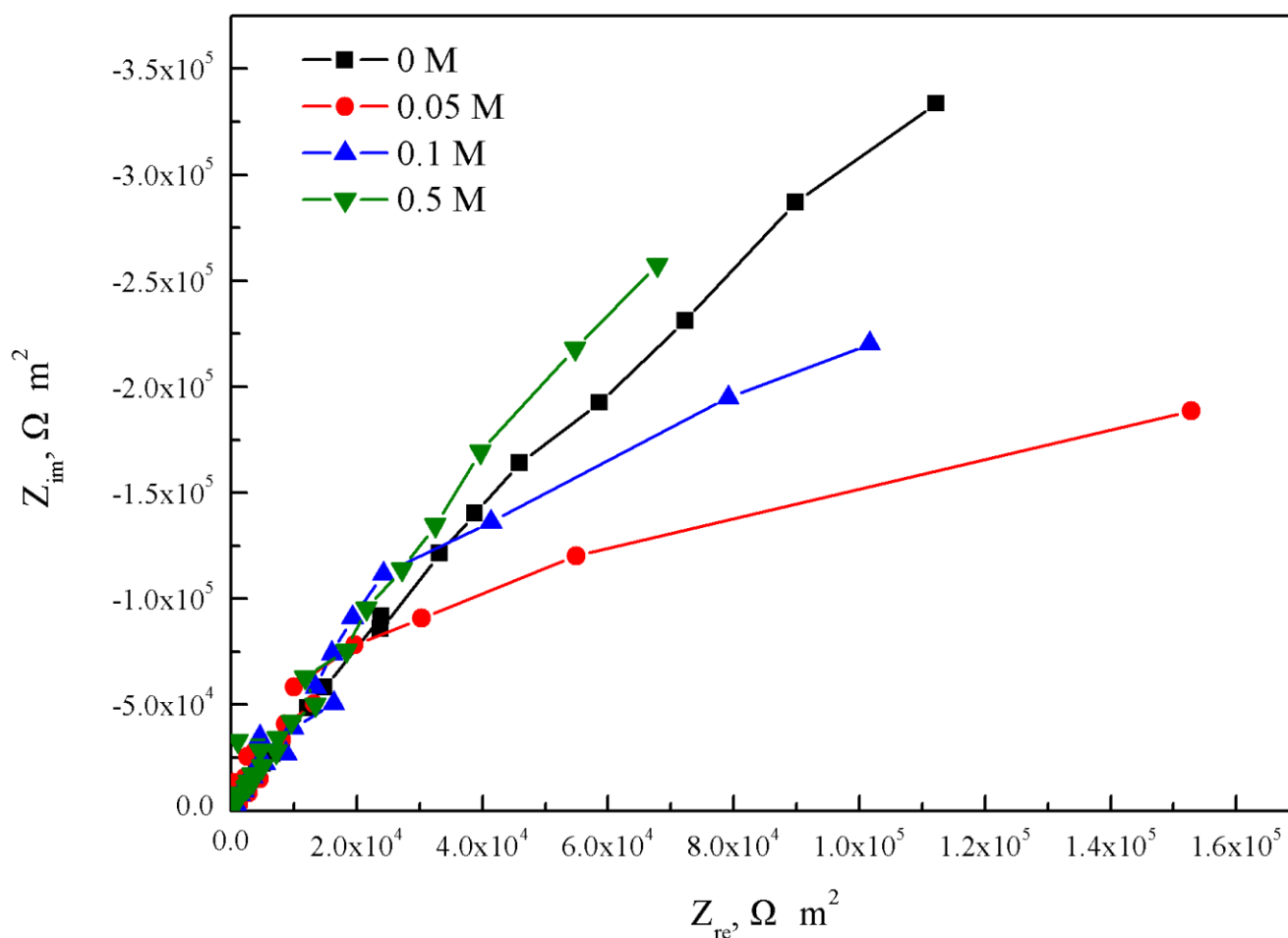

Figure 2. Nyquist diagrams of the passive films on duplex stainless steel 2205 formed at 0.2 V_{SCE} for 2 h in 3.5 wt.% chloride solution containing various concentrations of thiosulfate

However, as the concentration of $Na_2S_2O_3$ continued to increase, the radius of the semicircular capacitive arc also continued to increase. It is well known that the radius of the semicircular arc of the Nyquist curve represents the magnitude of the impedance of the passive film. That is, the greater the magnitude the better the resistance. Changes in the magnitude are related to the corrosion resistance of the passive film. The addition of 0.05 M $Na_2S_2O_3$ to the 3.5 wt.% NaCl solution showed a decrease in the overall impedance values, indicating a deterioration of the corrosion resistance. This corresponded well with the potentiodynamic polarization curves. Various different models had been suggested to interpret impendence spectra on passive surfaces. The two time constant *R-Q (CPE)* elements connected in series with the solution resistance R_s equivalent circuit in Figure 3 was adopted for this measurement [21]. In the first process *($R_1(CPE_1)$)* at higher frequencies, CPE_1 represents the capacitance of the passive film, consisted with the resistance of the ionic paths through the oxide film R_1. In the second process at lower frequencies, CPE_2 is correlated to the capacitance of the interfaces and R_2 for the corresponding charge-transfer resistance. *CPE* has been generally used for modeling frequency dispersion behavior corresponding to different physical phenomena. *CPE* is defined in impedance representation as [22]:

$$Z = Z_0 \cdot (i\omega)^{-n} \tag{1}$$

where Z_0 is the *CPE* constant, ω is the angular frequency, $i^2 = 1$ is the imaginary number, n is the exponent of the *CPE* with a value from 0 to 1. When $n = 0$, *CPE* represents resistance, when $n = 1$, *CPE* represents capacitance and when $n = 0.5$, *CPE* is the Warburg impedance.
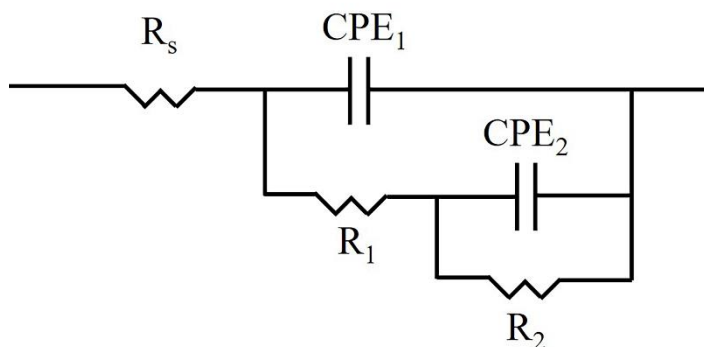

Figure 3. The electrochemical equivalent circuit for passive films on duplex stainless steel 2205

R_p ($R_p = R_1+R_2$, with R_1 and R_2 being parameters of the fitting results) reflects the polarization resistance and is utilized as a measure of the film dissolution resistance. Figure 4 presents R_p as a function of the concentration of thiosulfate. The higher the R_p value, the better the corrosion resistance capability [15,23]. The addition of 0.05 M thiosulfate apparently decreased the R_p by approximately 20 kΩ·cm^2, and a further increase in the thiosulfate level leads to a slight increase in the R_p. These results suggest that a small amount addition of thiosulfate accelerates the dissolution of the passive film, which is consistent with the findings of Faichuk [24].
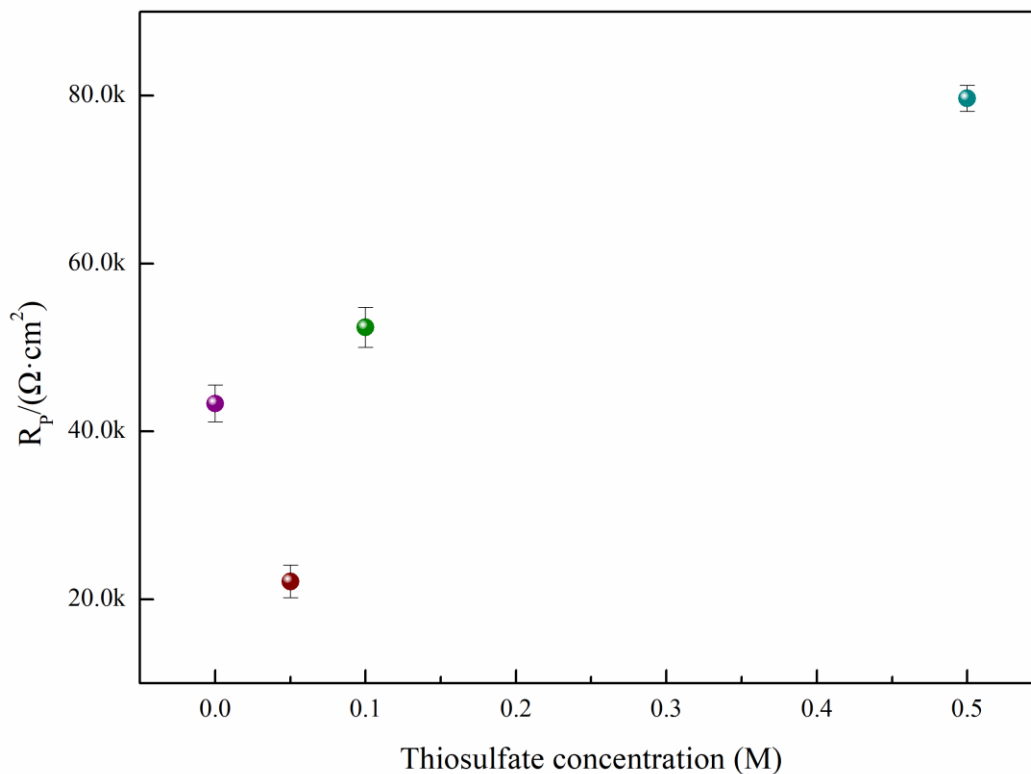
Figure 4. Calculated R_p values of duplex stainless steel 2205 in 3.5 wt.% NaCl solution containing various concentrations of thiosulfate

After the values were obtained, the capacitance related to the *CPE* could be calculated by the following equation [25]:

$$C = \frac{(QR)^{1/n}}{R} \tag{2}$$

where Q (*CPE*) is a constant phase element, n is the exponent of the *CPE*, and R is the resistance of the passive film. This can be used to estimate the thickness of the passive film, which is valid for the parallel-plate capacitor model of a homogeneous oxide layer. The thickness of the passive film was measured using the following relation [25]:

$$d = \frac{\varepsilon \varepsilon_0 A}{C} \tag{3}$$

where d is the thickness of the passive film, ε is the dielectric constant, ε_0 is the permittivity of vacuum 8.85×10^{-12} Fm^{-1}, A is the effective area, and C is the capacitance. However, accurate values of the passive film thickness are hard to obtain using capacitance because the dielectric constant is generally not well known and may vary with the composition of the passive films. The estimated values of d indicated that the films formed are typically a few nanometers thick in the 3.5 wt.% NaCl solutions containing different concentrations of $Na_2S_2O_3$.

When the concentration of $S_2O_3^{2-}$ in the Cl^- solution was low, the aggressive ions of the solution were mainly determined by the Cl^- ions. Once the passive film was broken down and metastable pitting

was initiated, the adsorbed $S_2O_3^{2-}$ ions on the fresh bare metal inhibited the repassivation of the film [8]. As a result, the thickness of the passive film was decreased compared to that of the Cl^--only solution. Therefore, the corrosion resistance of the film was reduced, and the protective ability was deteriorated [26]. The detrimental effect of very low concentrations of thiosulfate on a passive film in chloride solution was observed even though the specimen was in a well-passivated state. When the concentration of $Na_2S_2O_3$ was higher, the corrosion of the solution was decided by $S_2O_3^{2-}$ ions, and the adsorption of $S_2O_3^{2-}$ on the surface of the stainless steel acted as an inhibition to Cl^-. The harmful effect of Cl^- on duplex stainless steel was decelerated by $S_2O_3^{2-}$, and the corrosion resistance of the passive film was excellent. Therefore, the detrimental effect depended on the concentration ratio of thiosulfate to chloride in the service environment [27,28].

3.3 Mott-Schottky Analysis

The corrosion resistance of stainless steel in aggressive service environments is mainly determined by the passive film on the surface. The oxide films are semiconductors. The semiconductor characteristics of the passive films on duplex stainless steel 2205 formed in chloride solution containing different concentrations of thiosulfate were investigated by Mott-Schottky measurements. The relationship between capacitance behavior and the applied potential is provided by the classical Mott-Schottky equation, which depicts the potential dependence of the space charge capacitance, C, of a semiconductor electrode under the depletion condition [29-31]:

$$\frac{1}{C^2} = \pm \frac{2}{\varepsilon \cdot \varepsilon_0 \cdot e \cdot N} (E - E_{FB} - \frac{kT}{e}) \qquad (4)$$

where ε is the relative dielectric constant of the semiconductor with a value is 15.6 for stainless steel, ε_0 is the vacuum permittivity, e is the electron charge, N is the charge carrier density (electron donor density (N_A) for n-type semiconductor or acceptor density (N_D) for p-type semiconductor), k is the Boltzmann constant and T is the absolute temperature. E is the electrode applied potential and E_{FB} is the flat-band potential. A positive slope indicates n-type and a negative slope indicates p-type semiconductor behavior. The value of N_A can be determined from the slope of the experimental C^{-2} vs E. According to (4), the slopes of the linear portion of C^{-2} vs E give the charge carrier density N, from the following relation [32]:

$$N = \frac{2}{m \cdot e \cdot \varepsilon \cdot \varepsilon_0} \qquad (5)$$

where m is the slope of the Mott-Schottky plot in the linear region of interest, e is the electron charge, ε the relative dielectric constant of the semiconductor, and ε_0 is the vacuum permittivity.

Figure 5 displays the Mott-Schottky curves of the films on duplex stainless steel 2205 formed in 3.5 wt.% NaCl solution containing various concentrations of thiosulfate. The plots were divided into three intervals according to the slope of the linear portion. The potential region I and III, with positive slopes, revealed that the passive films exhibited n-type semiconductor characteristics. For the potential region II, the negative slope holds for p-type semiconductors. Numerous studies have shown that the passive films on stainless steel are primarily composed of chromium oxide and iron oxide [23,31,33-34]. Thence, the three regions of the Mott-Schottky curve indicated that there may be divalent and trivalent iron and trivalent chromium oxides in the passive film on duplex stainless steel. In region I, the

capacitive characteristics of the film were controlled by Fe(III) oxides. Since the iron oxides reveal an n-type semiconductor behavior, the slope of the linear portion of the Mott-Schottky plots was positive. In region II, the capacitance was dominated by Cr(III) oxides. Since the Cr(III) oxides are p-type semiconductors, the slope was negative in this region. In the potential region III, the capacitive response of the film was produced by Fe(II) oxides. Since Fe(II) oxides are n-type semiconductors, the slope was reflected as positive.
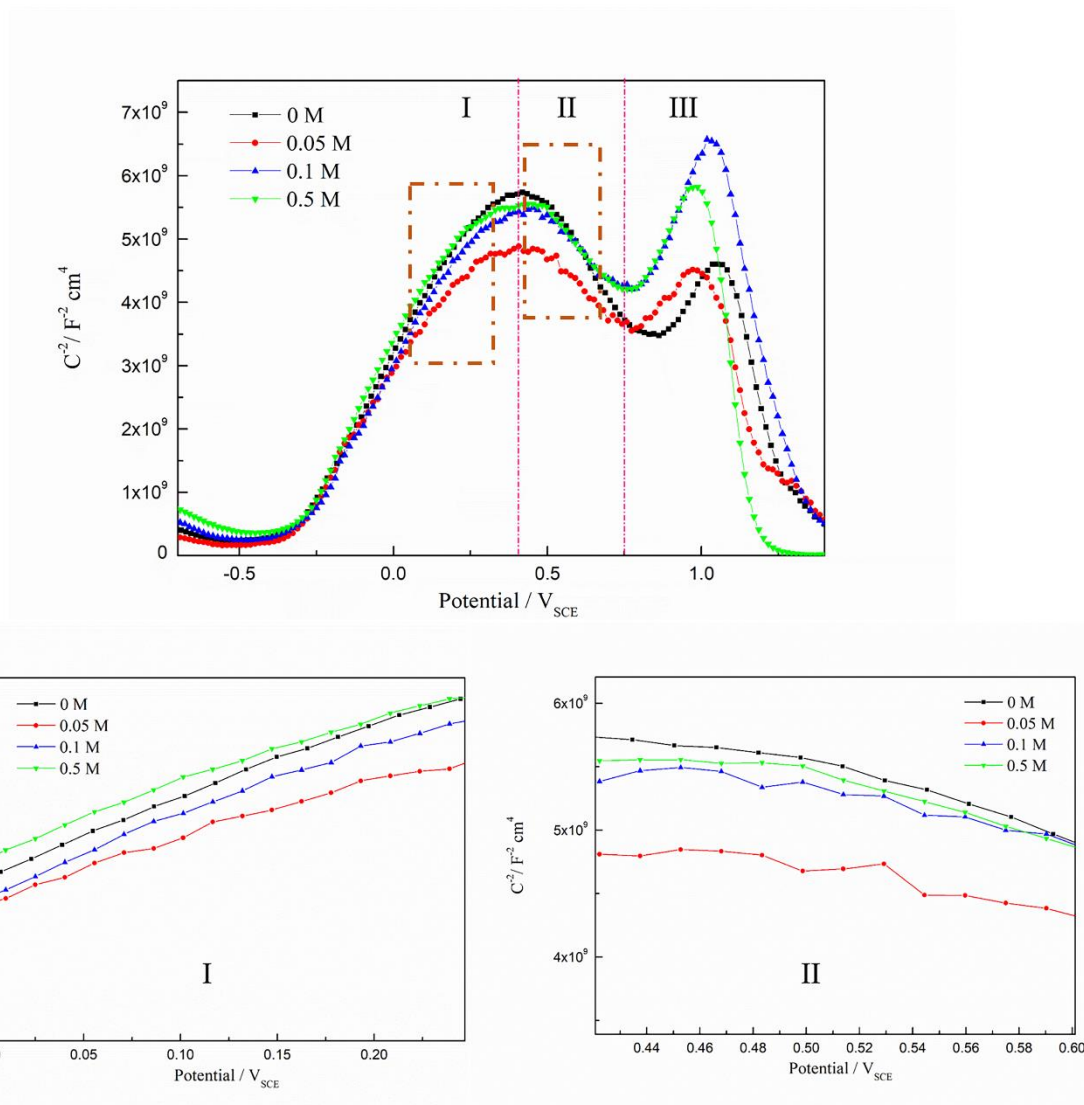

Figure 5. Mott-Schottky plots of passive films on duplex stainless steel 2205 formed at 0.2 V_{SCE} for 2 h in 3.5 wt.% NaCl solution containing various concentrations of $S_2O_3^{2-}$

According to the Mott-Schottky curves, two characteristics can be indicated when comparing the results in chloride solution with different concentrations of thiosulfate. First, the semiconductor type was not influenced by the addition of thiosulfate. Second, the donor and acceptor densities were modified with increasing thiosulfate content. In region I, the slopes of the curves first decreased and then increased with the increasing concentration of $Na_2S_2O_3$, which revealed that the donor densities in the passive film

first increased and then decreased accordingly. This result corresponded to the electrochemical impedance spectroscopy of the passive film on duplex stainless steel 2205 in Cl^- solution with various concentrations of $S_2O_3^{2-}$ ions. In the case of a low concentration of $S_2O_3^{2-}$, the solution was highly aggressive due to a relatively high concentration of Cl^- ions, resulting in a high density of impurities and more internal defects in the film. However, as the concentration of $Na_2S_2O_3$ increased, the aggressive anions in the solution were dominated by $S_2O_3^{2-}$, the corrosion of the solution became mild, and the impurity density in the passive film was reduced. In region II, the performance of the passive film was dominated by Cr(III). The Mott-Schottky curve of the passive film formed in the Cl^--only solution showed the largest slope, indicating the smallest defect density in the film. It is suggested that the presence of $S_2O_3^{2-}$ promotes the oxidation of Cr(III) to Cr(IV), causing a reduction of the corrosion resistance of the passive film at high potential [15]. In region III, the passive film was effected by Fe(II) oxide, and the addition of $S_2O_3^{2-}$ led to an increase in the slope, indicating that the chromium oxide was dissolved and the proportion of iron oxide increased, but that the density of defects in the film decreased. This, combined with the results of electrochemical impedance spectroscopy that the impedance magnitude of the passive film was lower than that in the Cl^--only solution when the concentration of $S_2O_3^{2-}$ was low, revealed that the corrosion resistance of the passive film was dependent primarily on chromium oxides.
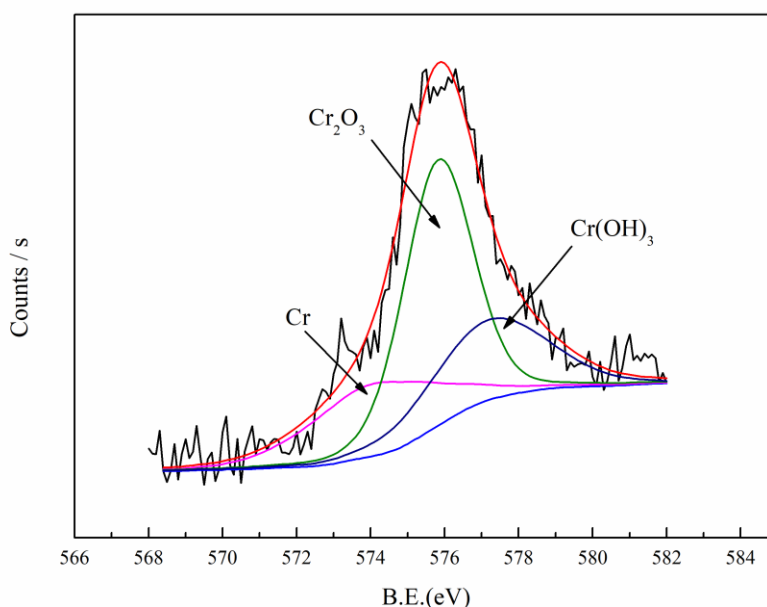
3.4 X-ray Photoelectron Spectroscopy Analysis

Figure 6. The XPS detailed spectra of Cr $2p_{3/2}$ of the passive film on duplex stainless steel 2205 formed at 0.2 V_{SCE} for 8 h in 3.5 wt.% NaCl solution containing 0.05 M $Na_2S_2O_3$

The composition determines the stability and corrosion resistance of the passive film. The chemical composition of the passive film formed on the duplex stainless steel 2205 in 3.5 wt.% NaCl

containing 0.05 M $Na_2S_2O_3$ solution at the formation potential of 0.2 V_{SCE}, which is a well-passivated potential, was analyzed by XPS measurements. Figures 6-10 display the XPS spectra and the fitting results of the high-resolution Cr $2p_{3/2}$, Fe $2p_{3/2}$, Mo $3d_{5/2}$, Ni $2p_{3/2}$ and O 1s on duplex stainless steel 2205. After background subtraction according to Shirley, each element was separated into contributions of different oxidation states.
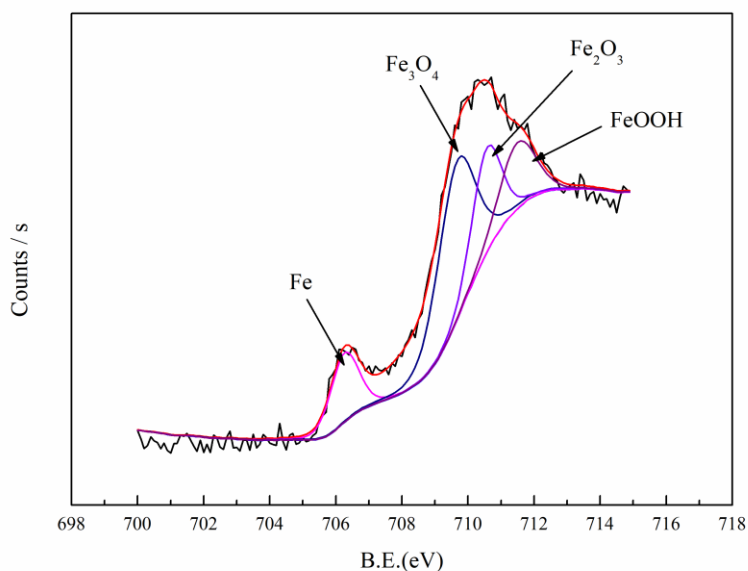

Figure 7. The XPS detailed spectra of Fe $2p_{3/2}$ of the passive film on duplex stainless steel 2205 formed at 0.2 V_{SCE} for 8 h in 3.5 wt.% NaCl solution containing 0.05 M $Na_2S_2O_3$
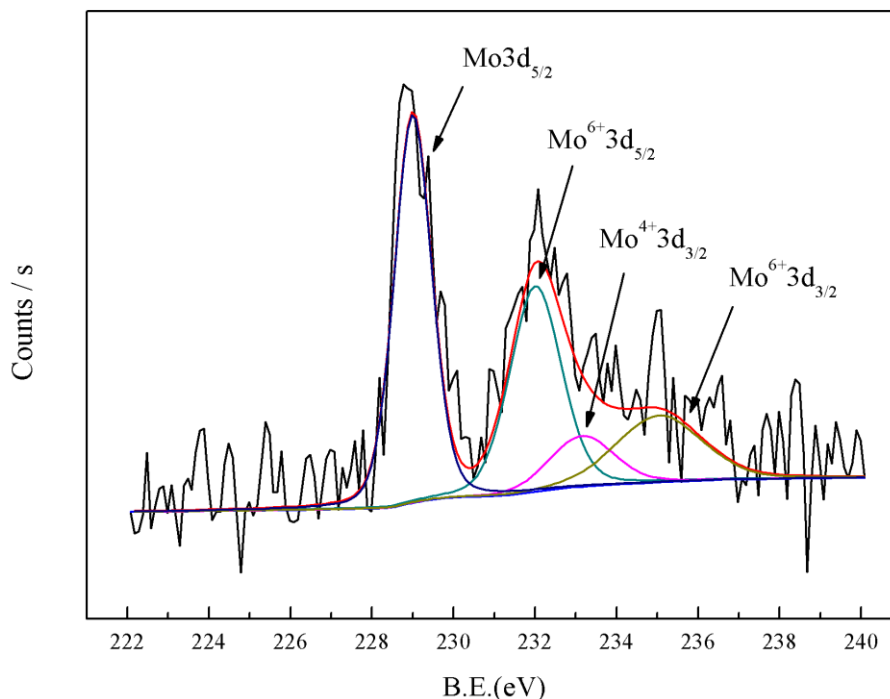

Figure 8. The XPS detailed spectra of Mo 3d of the passive film on duplex stainless steel 2205 formed at 0.2 V_{SCE} for 8 h in 3.5 wt.% NaCl solution containing 0.05 M $Na_2S_2O_3$

According to the binding energies, the chromium profile revealed that there are mainly three constituent peaks representing the metallic state Cr^0 (574.3 eV), Cr_2O_3 (576.3 eV) and $Cr(OH)_3$ (577.1 eV) [35,36]. It can be seen that the oxide species are the primary chemical components of the passive films on duplex stainless steel 2205. The chromium in the oxide layer plays quite an important role in the corrosion resistance and the electrochemical behavior of the passive film. The spectra of Fe $2p_{3/2}$ show several constituent peaks corresponding to the metallic Fe^0 (707.7 eV), Fe^{2+} and Fe^{3+} species. The relative peaks of FeO (709.4 eV) and Fe_2O_3 (710.9 eV) indicate that the Fe^{2+} and Fe^{3+} species were in the iron oxides in the passive films [3]. A relatively low-intensity Mo $3d_{5/2}$ and $3d_{3/2}$ spectrum is recorded and represents metallic Mo^0 (227.4 eV), Mo^{4+} (233.4 eV), and hexavalent Mo^{6+} (235.1 eV) species [5]. It is inferred that Mo^{6+} is the main molybdenum oxide species in the passive film. The Ni $2p_{3/2}$ spectra represented the metallic state Ni^0 (852.8 eV), NiO (854.3 eV) and $Ni(OH)_2$ (855.6 eV) [5,15]. The O 1s signal indicated three different components as well. The oxygen species O^{2-} and OH^- of the passive film act as metal ion connections. The peak at 530.2 eV was a result of an anhydrous oxide species, M-O (M being the alloy element), whereas the peak at 531.8 eV was characteristic of the hydrated oxide species, M-OH. The final peak at 533 eV was the residual water on the specimen surface. Additionally, the spectra for S 2p were also scanned, but no obvious peaks were detected in the passive film.

The results reveal that the primary components of the passive film on duplex stainless steel 2205 in the Cl^--$S_2O_3^{2-}$ solution were Cr-oxides and Fe-oxides and hydroxides with small amounts of Ni-oxides and Mo-oxides.

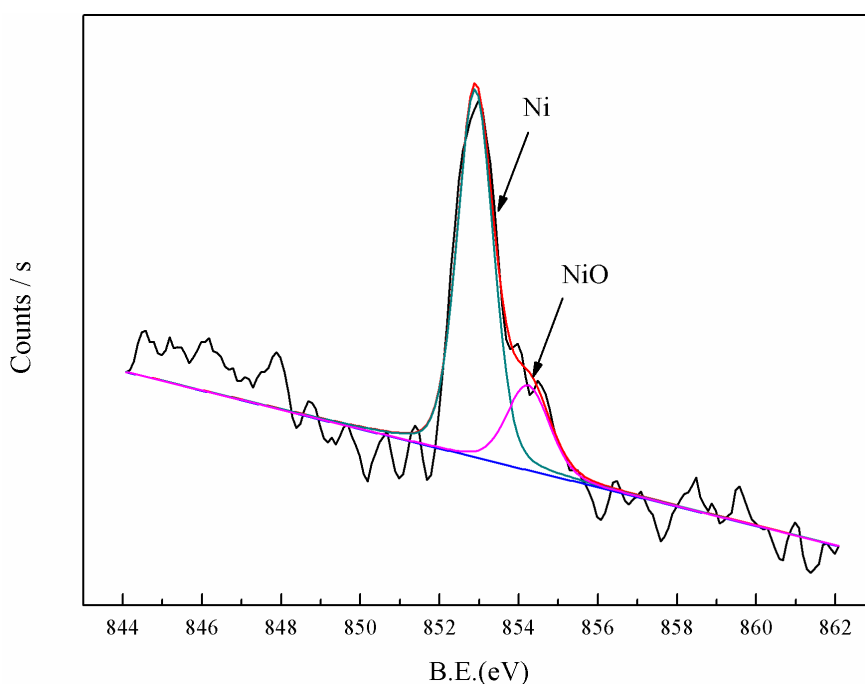**Figure 9.** The XPS detailed spectra of Ni $2p_{3/2}$ of the passive film on duplex stainless steel 2205 formed at 0.2 V_{SCE} for 8 h in 3.5 wt.% NaCl solution containing 0.05 M $Na_2S_2O_3$
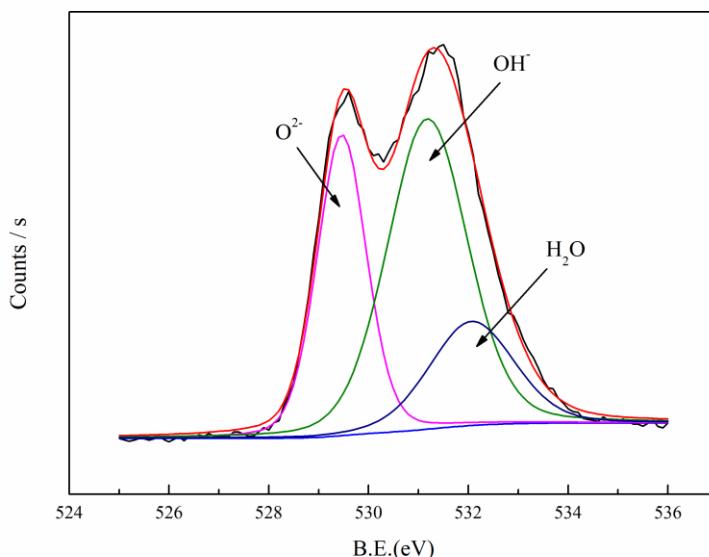
Figure 10. The XPS detailed spectra of O 1s of the passive film on duplex stainless steel 2205 formed at 0.2 V_{SCE} for 8 h in 3.5 wt.% NaCl solution containing 0.05 M $Na_2S_2O_3$

4. CONCLUSIONS

The corrosion and passive behavior of duplex stainless steel 2205 in 3.5 wt.% NaCl containing various concentrations of thiosulfate have been investigated in this work. The main conclusions obtained are presented below:

The addition of $S_2O_3^{2-}$ to a neutral 3.5 wt.% NaCl solution modified the breakdown potential of duplex stainless steel 2205. The detrimental effect depended on the concentration ratio of thiosulfate to chloride in the service environment. The Cl^- and $S_2O_3^{2-}$ competed for adsorption on the surface of the stainless steel at lower potentials, but a synergistic effect that promoted the dissolution of the passive films at higher potentials was also detected.

The presence of thiosulfate significantly affected the electrochemical impedance spectroscopy of passive films on stainless steel. When the concentration of $S_2O_3^{2-}$ in the Cl^- solution was low, the corrosion resistance and protective ability was deteriorated compared to the Cl^--only solution. When the concentration of $Na_2S_2O_3$ was higher, the harmful effect of Cl^- on duplex stainless steel was decelerated by $S_2O_3^{2-}$ and the corrosion resistance of the passive film was excellent.

The passive films on the duplex stainless steel 2205 in the Cl^--$S_2O_3^{2-}$ solutions exhibited n-type and p-type semiconductor characteristics. The concentration of $S_2O_3^{2-}$ had no effect on the semiconductor type of passive films but influenced the donor and acceptor densities.

The primary components of the passive films on duplex stainless steel 2205 in $S_2O_3^{2-}$ solutions were Cr-oxides and Fe-oxides or hydroxides with small amounts of oxides of Ni and Mo.

References

1. D. Han, Y. Jiang, C. Shi, B. Deng, J. Li, *J Mater Sci.*, 47 (2012) 1018.
2. Y. Wang, P. Singh, *Corrosion.*, 71 (2015) 184.
3. C. Abreu, M. Cristóbal, R. Losada, X. Nóvoa, *Electrochim. Acta.*, 49 (2004) 3049.
4. C. ÖrnekD, L. Engelberg, *J Mater Sci.*, 51 (2016) 1931.
5. H. Luo, C. Dong, K. Xiao, X. Li, *Appl. Surf. Sci.*, 258 (2011) 631.
6. F. Zanotto, V. Grassi, A. Balbo, C. Monticelli, F. Zucchi, *Corros. Sci.*, 80 (2014) 205.
7. M. Moradi, Z. Song, L. Yang, J. Jiang, J. He, *Corros. Sci.*, 84 (2014) 103.
8. L. Choudhary, D. Macdonald, A. Alfantazi, *Corrosion.*, 71 (2015) 1147.
9. A. Almarshad, D. Jamal, *J. Appl. Electrochem.*, 34 (2004) 67.
10. J. Lv, H. Luo, *J. Mater. Eng. Perform*, 23 (2014) 4223.
11. H. Kuo, H. Chang, W. Tsai, *Corros. Sci.*, 41 (1999) 669.
12. D. Nakhaie, M. Zakeri, M. Naghizadeh, M. Moayed, *J. Electrochem. Soc.*, 162 (2015) C121.
13. Z. Cui, S. Chen, L. Wang C. Man, Z. Liu, J. Wu, X. Wang, S. Chen, X. Li, *J. Electrochem. Soc.*, 164 (2017) C856.
14. D. Xia, Y. Sun, S. Chen, *Corros. Sci.*, 100 (2015) 504.
15. S. Wu, J. Wang, S. Song, D. Xia, Z .Zhang, Z. Gao, J. Wang, W. Jin, W. Hu, *J. Electrochem. Soc.*, 164 (2017) C94.
16. M. Kappes, G. Frankel, R. Thodla, M. Mueller, N. Sridhar, Carranza, *Corrosion.*, 68 (2012) 1015.
17. D. Xia, R. Zhu, Y. Behnamian, J. Luo, C. Lin, S. Klimas, *J. Electroanal. Chem.*, 744 (2015) 77.
18. D. Xia, S. Song, R. Zhu, Y. Behnamian, C. Shen, J. Wang, J. Luo, Y. Lu, S. Klimas, *Electrochim. Acta*, 111 (2013) 510.
19. Y. Liou, S. Chiu, C. Lee, H. Shih, *J. Appl. Electrochem.*, 29 (1999) 1377.
20. H. Tian, X. Wang, Z. Cui, Q. Lu, L. Wang, L. Lei, Y. Li, D. Zhang, *Corros. Sci.*, 144 (2018) 145.
21. M. Mohammadi, L. Choudhary, I. Gadala, A. Alfantazi, *J. Electrochem. Soc.*, 163 (2016) C883.
22. A. Igual Munoz, J. Garcıa Anton, J. Guinon, V. Perez Herranz, *Corros. Sci.*, 49 (2007) 3200.
23. H. Luo, C. Dong, X. Li, K. Xiao, *Electrochim. Acta*, 64 (2012) 211.
24. M. Faichuk, S. Ramamurthy, W. Lau, *Corros. Sci.*, 53 (2011) 1383.
25. P. Girault, J. Grosseau-Poussard, J. Dinhut, L. Marechal, *Nucl. Phys. B.*, 174 (2001) 439.
26. T. Laitinen, *Corros. Sci.*, 42 (2000) 421.
27. D. Nakhaie, M. Zakeri, M. Naghizadeh, M. Moayed, *J. Electrochem. Soc.*, 162 (2015) C121.
28. W. Tsai, T. Wu, *J. Nucl. Mater.*, 277 (2000) 169.
29. J. Dewald, *J. Phys. Chem. Solids.*, 14 (1960) 155.
30. W. Gomes, D. Vanmackelbergh, *Electrochim. Acta.*, 41 (1996) 967.
31. R.M. Fernández-Domene, E. Blasco-Tamarit, D.M. García-García, J. García-Antó, *Thin Solid Films*, 558 (2014) 252.
32. L. Hamadou, A. Kadri, N. Benbrahim, *Corros. Sci.*, 52 (2010) 859.
33. C. Sunseri, *J. Electrochem. Soc.*, 137 (1990) 2411.
34. R.Sánchez-Tovar, R. Leiva-García, J. García-Antón, *Thin Solid Films*, 576 (2015) 1.
35. N. Padhy, Ranita Paul, U. Kamachi Mudali, Baldev Raj, *Appl. Surf. Sci.*, 257 (2011) 5088.
36. V. Shankar Rao, L. Singhal, *J. Mater. Sci.*, 44 (2009) 2327.